

## Effects of anodic titanium dioxide nanotubes of different diameters on macrophage secretion and expression of cytokines and chemokines

W. L. Lü\*†, N. Wang\*, P. Gao†, C. Y. Li†, H. S. Zhao‡ and Z. T. Zhang\*

\*School of Stomatology, Capital Medical University, Beijing, 100050, China, †Hospital and School of Stomatology, Tianjin Medical University, Tianjin, 300070, China and ‡Center for Stem Cell and Tissue Engineering, School of Medicine, Zhejiang University, Zhejiang Province, 310058, China

Received 14 August 2014; revision accepted 21 August 2014

### Abstract

**Objectives:** To investigate effects of TiO<sub>2</sub> nanotubes of different diameters on J744A.1 macrophage behaviour, secretion and expression of pro-inflammatory cytokines and chemokines.

**Materials and methods:** Macrophage-like J744A.1 cells were cultured on three types of Ti surface: mechanically polished titanium plus 30 and 80 nm TiO<sub>2</sub> nanotube surfaces, for 4, 24 and 48 h. Macrophage adhesion and proliferation were assessed using CCK-8 assay. Levels of pro-inflammatory cytokines (TNF- $\alpha$ , IL-1 $\beta$  and IL-6) and chemokines (MCP-1 and MIP-1 $\alpha$ ) secreted into the supernatant were measured using the Cytometric Bead Arrays kit. *TNF- $\alpha$* , *MCP-1* and *MIP-1 $\alpha$*  gene expression were quantitatively analysed by real-time PCR.

**Results:** These show that TiO<sub>2</sub> nanotube surfaces, especially of 80 nm TiO<sub>2</sub> nanotube, benefited macrophage adhesion and proliferation, and reduced protein secretion and mRNA expression of TNF- $\alpha$ , MCP-1 and MIP-1 $\alpha$ . IL-1 $\beta$  and IL-6 were undetectable on all the surfaces at all times.

**Conclusions:** TiO<sub>2</sub> nanotube surfaces, especially of 80 nm TiO<sub>2</sub> nanotube, reduced inflammatory response *in vitro*, which might be part of a basis for rapid osseointegration in implants with TiO<sub>2</sub> nanotube surfaces in animal studies.

### Introduction

Insertion of a dental implant into osseous tissue immediately triggers an inflammatory response at the implant site

Correspondence: Z. T. Zhang, School of Stomatology, Capital Medical University, 4 Tiantanxili, Beijing, 100050, China. Tel.: +86 10 67099007; Fax: +86 10 67099310; E-mail: zzttx1@hotmail.com

(1,2). Macrophages are among the first cells to arrive at the tissue–implant interface and have, for a long time, been recognized as key players in inflammation and wound healing (3,4). They clear cell debris and begin to produce growth factors, chemokines and cytokines, which can influence progression of subsequent both inflammatory and healing events (1–4). Recent studies indicate that macrophages have remarkable functional plasticity and, thus, can play both positive and negative roles in tissue remodelling (5). For example, macrophages produce bone morphogenetic protein-2 (6,7), transforming growth factor-beta (TGF- $\beta$ ) (8) as well as vascular endothelial growth factor (1,9), all of which are important modulators of wound healing. In addition, macrophages also produce pro-inflammatory cytokines such as tumour necrosis factor-alpha (TNF- $\alpha$ ) and chemokines such as monocyte chemoattractant protein-1 (MCP-1). TNF- $\alpha$ , at low levels, can promote wound healing by indirectly stimulating inflammation and increasing macrophage growth factors. However, at higher levels, specially over prolonged periods of time, TNF- $\alpha$  has a detrimental effect on healing (10). Both MCP-1 and MIP-1 $\alpha$  have monocyte chemotactic activity and play key roles in immunoregulatory and inflammatory processes. MCP-1 and MIP-1 $\alpha$  also play a critical role in recruiting immune cells such as lymphocytes and monocytes to the implant site, promoting inflammation (11,12). Thus, reducing secretion of pro-inflammatory cytokines and chemokines by macrophages may contribute to rapid bone wound healing after dental implantation.

Currently, a great deal of effort is devoted to promoting rapid osseointegration around dental implants by changing implant surface characteristics such as its chemistry and topography (13). Surface topography of dental implants is a crucial factor that affects rate and extent of osseointegration (13). Many studies have suggested that titanium surface topography, especially at the microscale level, influence bone as well as the immune response, resulting in altered secretion of cytokines and

growth factors by macrophages, *in vitro* and *in vivo* (14–16). Latest pieces of research in surface modification of dental implants have been focused on topographies organized specifically at the nanometre scale (13,17). The rationale behind this change is that nanoscale modification may contribute to mimicry of cellular environments in favour of processes of rapid bone accrual (13,17). Meanwhile, nanoscale surface topographies may also have effects on the immune response (18–21). It can be hypothesized that macrophages recognize nanoscale surface topographies and respond accordingly by altered secretion of cytokines and chemokines; this results in promotion of the osseointegration process.

Among common surface nanotopographies, the titanium dioxide (TiO<sub>2</sub>) nanotubular surface has received considerable attention. TiO<sub>2</sub> nanotubes can be fabricated easily by anodization in a simple and economical way, and nanotube dimensions can be precisely controlled (22). *In vitro* studies have demonstrated that TiO<sub>2</sub> nanotubes can provide good attachment for osteoblasts, with suitable differentiation and osteoblastic gene expression (23–26). *In vivo*, TiO<sub>2</sub> nanotube implant surfaces increase new bone formation, bone bonding strength and bone-implant contact, specially during early stages of healing (27–29). However, up to now it has been unknown whether TiO<sub>2</sub> nanotubes of different diameters have any differing effects on macrophage responses. To better understand the adherent macrophage phenotype and its potential modulation by surface topography, we investigated effects of TiO<sub>2</sub> nanotubes of different diameters on macrophage behaviour, secretion and expression of pro-inflammatory cytokines and chemokines *in vitro*.

## Materials and methods

### *Fabrication of TiO<sub>2</sub> nanotubes*

The protocol for preparation of TiO<sub>2</sub> nanotubes by anodization is described as follows. Titanium disks, diameter of 15 mm, were cut from 0.6 mm thick sheets of commercially pure titanium (cp Ti; Ti > 99.7%, Baoji Titanium Industry Co., Ltd., Baoji, China). All disks were polished with SiC paper of successive grades from 100 to 600 grit, then ultrasonically cleaned in acetone, ethanol and distilled water respectively. Layers of TiO<sub>2</sub> nanotubes on a titanium surface were formed in 0.5% hydrofluoric acid solution at 5 and 20 V, for 1 h at room temperature, to obtain nanotubes with diameters of 30 and 80 nm. A platinum electrode (99.9%; Tianjin Aidahengsheng Technology Co., Ltd., Tianjin, China) served as cathode. To crystallize the as-deposited amorphous-structured TiO<sub>2</sub> nanotubes, specimens were heat

treated at 450 °C for 3 h. Identically sized mechanically polished titanium (PO Ti) disk was used as control after cleaning and sterilization. All the samples were sterilized by ultraviolet irradiation for 2 h.

### *Surface characterization*

Surface morphology of the TiO<sub>2</sub> nanotubes, before and after heat treatment, was observed by using a field-emission scanning electron microscope (S4800 FE-SEM; Hitachi, Tokyo, Japan). Phase composition of TiO<sub>2</sub> nanotubes, after heat treatment, was evaluated by X-ray diffractometry (D8 advance; Bruker AXS, Karlsruhe, Germany) using Cu K $\alpha$  radiation in the 2 $\theta$  range at 20–80°. Contact angle measurements were carried out by sessile-drop method on a contact angle measuring system (JC2000A; Shanghai Powereach Digital Company, Shanghai, China) at room temperature. One microlitre of ultra-pure water was employed in contact angle measurements. Contact angle was measured by analysing drop shape using the corresponding software (JC2000A; Powereach Digital, Shanghai, China).

### *Cell culture*

Mouse macrophage cell line J774A.1 was obtained from the Cell Resource Center, Institute of Basic Medical Sciences, Peking Union Medical College. Cells were cultured in Dulbecco's modified Eagle's medium (DMEM) supplemented with 10% foetal bovine serum (FBS) and 1% penicillin/streptomycin at 37 °C in humidified 5% CO<sub>2</sub> atmosphere. These were passaged every third day. Cells were then seeded onto the different titanium discs in 24-well polystyrene culture plates at  $2 \times 10^4$  cells per well. To analyse mRNA expression, cells were seeded onto each different titanium disk at  $1.5 \times 10^5$  cell/cm<sup>2</sup>.

### *Cell adhesion and proliferation*

After culturing for 4, 24 and 48 h, cell adhesion and proliferation were assessed using CCK-8 assay. At the prescribed time points, culture supernatants were harvested for cytokine and chemokine assays, centrifuged to remove particles (if any present), and stored at -80 °C. Then, specimens with seeded macrophages were rinsed with PBS and transferred to new 24-well culture plates. Subsequently, 1 ml of DMEM and 100  $\mu$ l of CCK-8 solution (Beyotime Biotechnology Institute, Haimen, China) were added to each sample. After 2 h incubation, 200  $\mu$ l of solution on each sample were transferred to a 96-well culture plate. Absorbance was measured at 450 nm using a microplate reader (Spectra

Max 386plus; Molecular Devices, Sunnyvale, CA, USA). Three parallel replicates of each sample, at each time point, were prepared during this cell adhesion and proliferation assay.

#### Secretion of cytokine and chemokine proteins

After culturing for 4, 24 and 48 h, culture supernatants were harvested for determination of secretion of cytokine and chemokine proteins. Cytokine (TNF- $\alpha$ , IL-1 $\beta$ , and IL-6) and chemokine (MCP-1 and MIP-1 $\alpha$ ) levels were measured in cell culture supernatants using Cytometric Bead Arrays (CBA) kit (BD Biosciences, San Jose, CA, USA) according to the manufacturer's instructions. A mouse CBA inflammation kit was used to simultaneously detect mouse TNF- $\alpha$ , IL-1 $\beta$ , IL-6, MCP-1 and MIP-1 $\alpha$ . In brief, a mixture of five capture bead populations (50  $\mu$ l) with distinct fluorescence intensities, coated with antibodies specific to the above cytokines and chemokines, was mixed with each sample/standard (50  $\mu$ l) and incubated for 1 h at room temperature. Additionally, PE-conjugated detection reagents were added to each assay tube to form sandwich complexes. After 1 h incubation in the dark, samples were washed once (200 g, 5 min) and resuspended in 300  $\mu$ l of wash buffer. The samples were acquired on a FACSAria Flow Cytometer (BD Biosciences) immediately. Fluorescence intensity was measured by flow cytometry, and quantified from a calibration curve using FCAP Array v1.0 Software (Softflow Technologies, New Brighton, MN, USA). Range of detection was 10–2500 pg/ml for each cytokine measured by CBA. All samples were assayed in triplicate at each time point.

#### Quantitative real-time PCR analysis

After culturing for 24 and 48 h, specimens with seeded macrophages were rinsed with PBS and transferred to new 24-well culture plates. Total cell RNA extraction was performed using TRIzol reagent (Invitrogen, Carlsbad, CA, USA). Quantity and quality of RNA obtained were analysed by UV 2000 spectrophotometry (Unico Shanghai Instrument Co., Ltd., Shanghai, China), according to the manufacturer's instructions. Extracted RNA was subsequently reverse-transcribed to cDNA using PrimeScript<sup>TM</sup>\_RT reagent kit (Takara Bio, Shiga, Japan). Gene-specific primers for TNF- $\alpha$ , MCP-1, MIP-1 $\alpha$  and endogenous housekeeping gene, GAPDH were commercially synthesized (Sun Biomedical Technology Co. Ltd., Beijing, China); specific primer sets are outlined in Table 1. Then, real-time PCR (Line-gene real time PCR detection system) was performed as follows: 45 cycles of 20 s at 95 °C, 25 s at 60 °C, 30 s at 72 °C after initial denatur-

**Table 1.** Sequences of the primers

Gene	Primer sequence (forward/reverse)	Product size (bp)
TNF- $\alpha$	5'-GTAGCCCACGTCGTAGCAAA-3' 5'-ACAAGGTACAACCCATCGGC-3'	137
MCP-1	5'-GAAGGAATGGGTCCAGACAT-3' 5'-ACGGGTCAACTTCACATTCA-3'	127
MIP-1 $\alpha$	5'-TCTGCGCTGACTCCAAAGAG-3' 5'-CTCAAGCCCCTGCTCTACAC-3'	130
GAPDH	5'-TTGCAGTGGCAAAGTGGAGA-3' 5'-GATGGGCTTCCCCTTGATGA-3'	154

ation step of 120 s at 95 °C using a mixture of BioEasy SYBR Green I, cDNA templates and each forward and reverse primers. Quantification of gene expression was based on  $C_T$  (threshold cycle) value of each measurement and was presented as average and standard deviation of three replicates.

#### SEM for analysis of cell morphology

After 4 h culture, cells on different samples were washed gently with PBS, fixed in 3% glutaraldehyde at 4 °C in PBS for 2 h, and post-fixed in 1% osmium tetroxide. Samples were then dehydrated in a graded series of alcohol (50, 70, 80, 90 and 100%) for 10 min each, dried in hexamethyldisilazane (HMDS) and coated with a thin layer of gold/palladium. Cell morphology was observed and recorded using scanning electron microscopy (TM-1000 SEM; Hitachi).

#### Statistical analysis

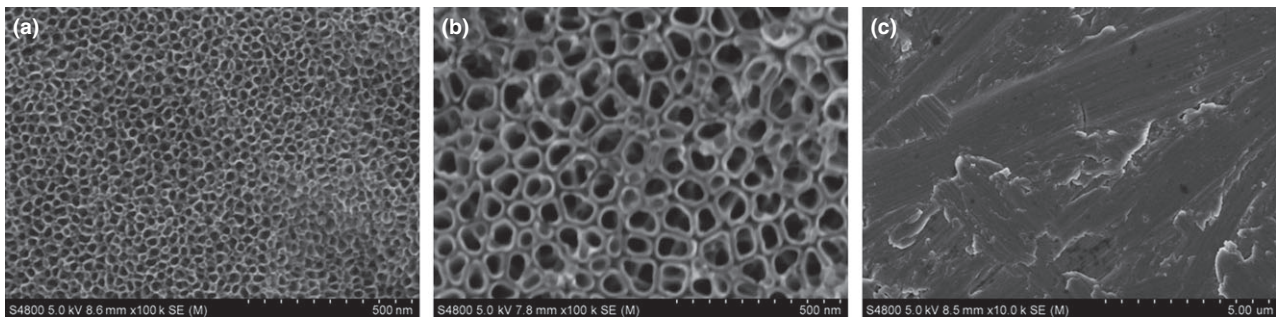
Average values presented from at least three sample sets for each time point. Error bars represent standard error mean. Statistical comparisons were determined using two-way analysis of variance (ANOVA) and *post hoc* Tukey multiple comparison testing. Significance level was set at  $P < 0.05$ .

## Results

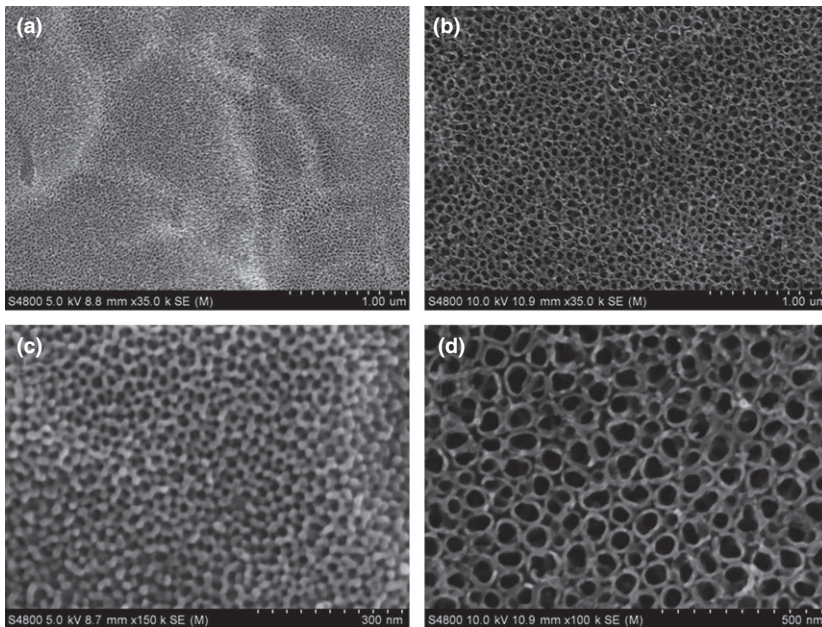
#### Surface characterization

Figure 1 is of SEM images of TiO<sub>2</sub> nanotube layers fabricated by anodization at 5 and 20 V for 1 h. As mentioned, diameters of TiO<sub>2</sub> nanotubes were altered by changing anodization potentials 5 and 20 V, to fabricate nanotubes of 30 and 80 nm respectively. 80 nm TiO<sub>2</sub> nanotube layer was found to be stable after heat treatment; no discernible changes in pore diameter nor wall thickness were observed after annealing at 450 °C for





**Figure 1.** Scanning electron microscope images of the various sample surfaces before heat treatment. (a) 30 nm (5 V) TiO<sub>2</sub> nanotube surface, (b) 80 nm (20V) TiO<sub>2</sub> nanotube surface and (c) mechanically polished Ti.



**Figure 2.** Scanning electron microscope images of TiO<sub>2</sub> nanotube surfaces after heat treatment. (a, c) 30 nm TiO<sub>2</sub> nanotube surface and (b, d) 80 nm TiO<sub>2</sub> nanotube surface.

3 h (Fig. 2b,d). However, the 30 nm TiO<sub>2</sub> nanotube layer was found to be unstable; surface morphologies changed (Fig. 2a,c), which as discovered in previous studies (30). Figure 3 shows XRD patterns of 30 and 80 nm TiO<sub>2</sub> nanotube samples annealed at 450 °C in dry oxygen ambient conditions. Heat-treated 80 nm TiO<sub>2</sub> nanotube layer was found to have anatase crystalline phase by x-ray diffractometer analysis (JCPDS card no. 21-1272). Intensity of anatase peaks of the 30 nm TiO<sub>2</sub> nanotube layer was not obvious, probably due to the thin TiO<sub>2</sub> layer.

Water contact angles were used to assess hydrophilicity of samples in this study (Fig. 4). There is a proportional relationship between contact angle and hydrophobicity of a material. The most hydrophobic sample was mechanically polished Ti, with water con-

tact angle of 53°. The most hydrophilic sample was 80 nm TiO<sub>2</sub> nanotubes, with water contact angle of 16° ( $P < 0.05$ ).

#### *Cell adhesion and proliferation*

As shown in Fig. 5, at all times, numbers of cells on the 80 nm TiO<sub>2</sub> nanotube surface were statistically higher than on the 30 nm TiO<sub>2</sub> nanotube and mechanically polished Ti surfaces ( $P < 0.05$ ).

#### *Secretion of cytokine and chemokine proteins*

Cytokine and chemokine secretion from the J744A.1 cells grown on different discs are shown in Fig. 6. At all times, TNF- $\alpha$  secreted by macrophages cultured on

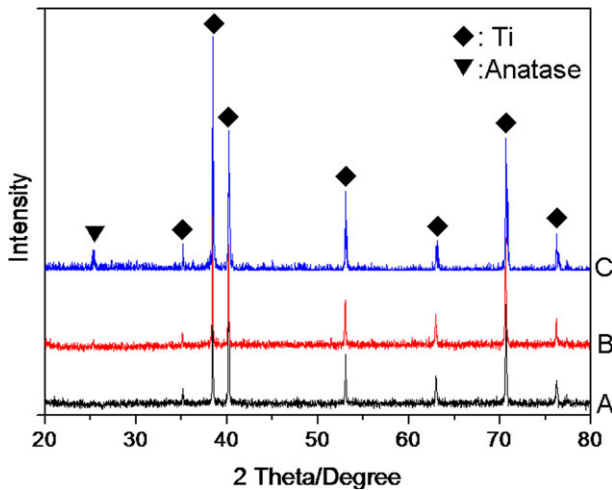


**Figure 3.** XRD patterns of the various sample surfaces. (a) mechanically polished Ti surface, (b) 30 nm TiO<sub>2</sub> nanotube surface and (c) 80 nm TiO<sub>2</sub> nanotube surface. ♦ denotes peaks for Ti, ▼ for anatase phase of TiO<sub>2</sub>.

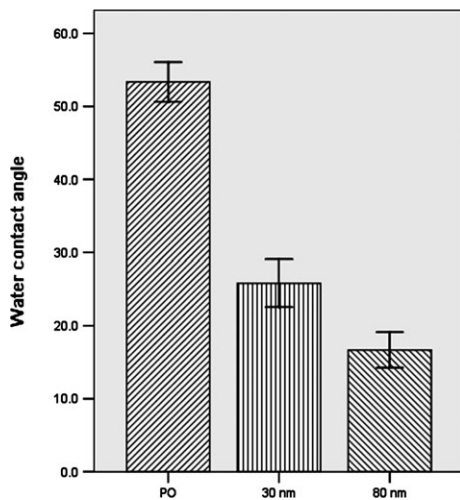


**Figure 4.** Contact angles (degrees) of the various samples. Error bars in the figure represent the standard deviation of nine specimens for each piece of data. \*Statistical significance ( $P < 0.05$ ).

mechanically polished Ti surface were significantly higher compared to 30 and 80 nm TiO<sub>2</sub> nanotube surfaces ( $P < 0.05$ ). After 4 h culture, TNF- $\alpha$  was almost undetectable on 30 and 80 nm TiO<sub>2</sub> nanotube surfaces, as shown in Fig. 6a.

IL-1 $\beta$  and IL-6 were undetectable in macrophage cultures on all surfaces at all times tested, which was consistent with previous reports (14).

After 4 h culture, differences in MCP-1 level produced by macrophages, among all the surfaces, were not statistically significant ( $P > 0.05$ ). However, after 24 and 48 h culture, level of MCP-1 produced by macrophages on the mechanically polished Ti surface was sig-

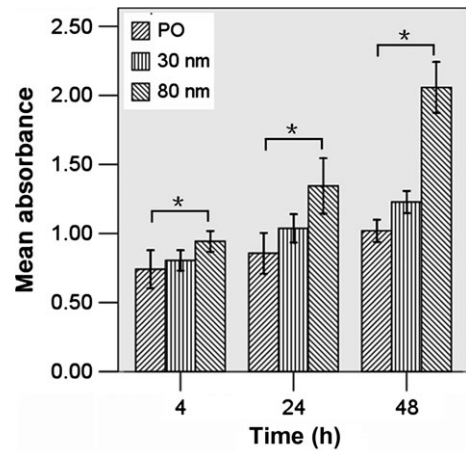


**Figure 5.** Macrophage adhesion and proliferation on the various sample surfaces by CCK-8 assay. Error bars represent standard deviation for three specimens for each piece of data. \*Statistical significance ( $P < 0.05$ ).

nificantly higher compared to 30 and 80 nm TiO<sub>2</sub> nanotube surfaces ( $P < 0.05$ ), as shown in Fig. 6b.

After 4 h culture, 30 and 80 nm TiO<sub>2</sub> nanotube surfaces were found to down-regulate MIP-1 $\alpha$  secretion of the macrophages compared to those of the mechanically polished Ti surface ( $P < 0.05$ ). After 24 h culture, level of MIP-1 $\alpha$  produced on 30 nm TiO<sub>2</sub> nanotube surface was significantly higher compared to mechanically polished Ti and 80 nm TiO<sub>2</sub> nanotube surfaces ( $P < 0.05$ ). However, after 48 h culture, differences in MIP-1 $\alpha$  level among all the surfaces, were not statistically significant ( $P > 0.05$ ), as shown in Fig. 6c.

#### TNF- $\alpha$ , MCP-1 and MIP-1 $\alpha$ mRNA levels

Levels of TNF- $\alpha$ , MCP-1 and MIP-1 $\alpha$  mRNA from macrophages grown on the different discs are shown in Fig. 7. After 24 and 48 h culture, TNF- $\alpha$  mRNA levels on 80 nm TiO<sub>2</sub> nanotube surfaces were significantly lower than those of mechanically polished Ti and 30 nm TiO<sub>2</sub> nanotube surfaces ( $P < 0.05$ ), as shown in Fig. 7a.

After 24 h culture, no significant difference was observed in MCP-1 mRNA expression among the three surfaces; however, after 48 h, MCP-1 mRNA expression on 80 nm TiO<sub>2</sub> nanotube surfaces were significantly lower than those on mechanically polished Ti and 30 nm TiO<sub>2</sub> nanotube surfaces ( $P < 0.05$ ), as shown in Fig. 7b.

After 24 and 48 h culture, levels of MIP-1 $\alpha$  mRNA on 30 and 80 nm TiO<sub>2</sub> nanotube surfaces were significantly lower than those on mechanically polished Ti surfaces ( $P < 0.05$ ), as shown in Fig. 7c.

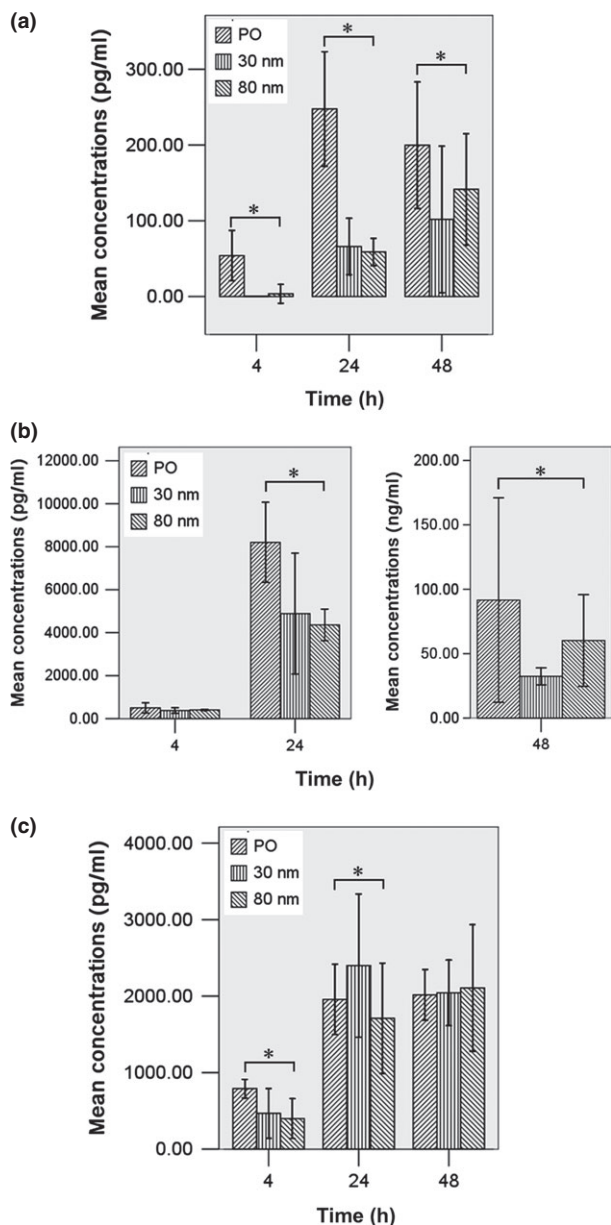


**Figure 6.** TNF- $\alpha$ , MCP-1 and MIP-1 $\alpha$  protein secretion by macrophages cultured on the various sample surfaces after 4, 24 and 48 h. (a) Concentration of TNF- $\alpha$ ; (b) Concentration of MCP-1; (c). Concentration of MIP-1 $\alpha$ . Error bars represent standard deviation for three specimens for each piece of data. \*Statistical significance ( $P < 0.05$ ).

### SEM of cell morphology

Scanning electron microscope images of macrophages cultured on the three different sample surfaces are presented in Fig. 8. On the mechanically polished Ti surface, more cells were nearly spherical with small protrusions visible on their surfaces. On the 30 and 80 nm TiO<sub>2</sub> nanotube surfaces, more cells had elongated

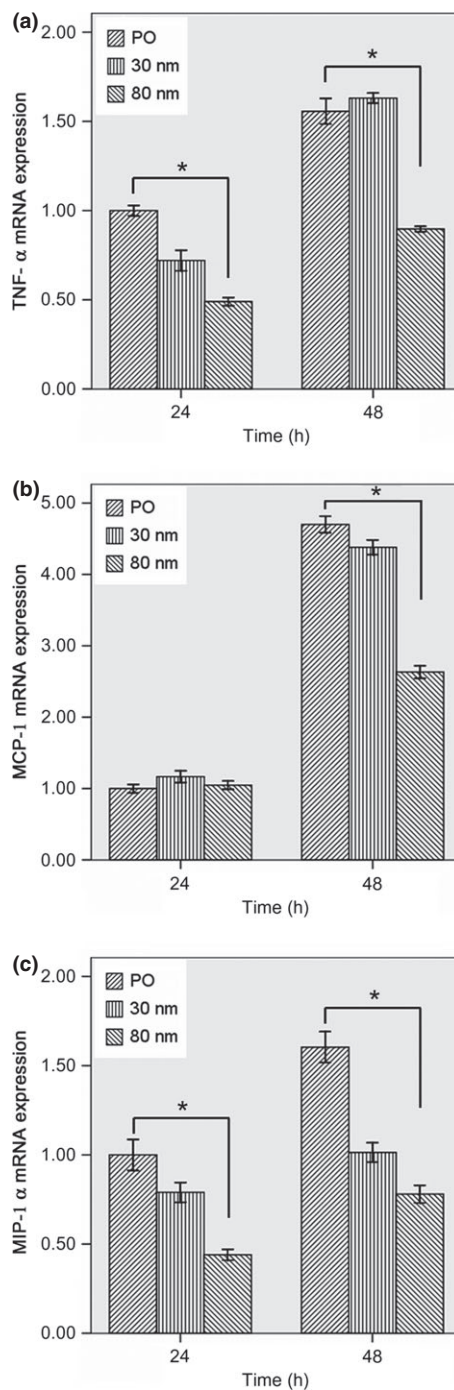


**Figure 7.** Evaluation of TNF- $\alpha$ , MCP-1 and MIP-1 $\alpha$  mRNA levels of macrophages cultured on the various sample surfaces after 24 and 48 h. (a) TNF- $\alpha$  mRNA expression; (b) MCP-1 mRNA expression; (c) MIP-1 $\alpha$  mRNA expression. Error bars represent the standard deviation for three specimens for each piece of data. \*Statistical significance ( $P < 0.05$ ).

morphology and were well spread out; this was because cells had numerous cytoplasmic protrusions/lamellipodia holding fast to sample surfaces.



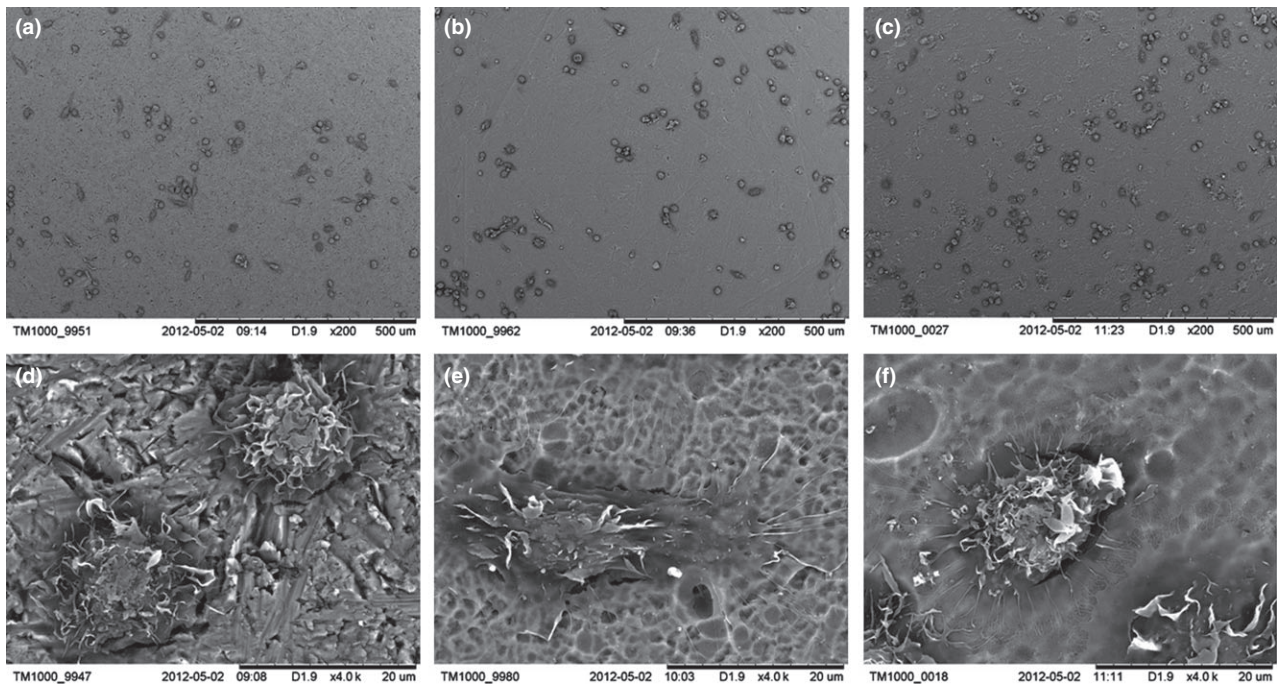


**Figure 8.** Scanning electron microscope images of macrophages cultured on the various sample surfaces for 4 h. (a, d) mechanically polished Ti surface, (b, e) 30 nm TiO<sub>2</sub> nanotube surface and (c, f) 80 nm TiO<sub>2</sub> nanotube surface.

## Discussion

Macrophages play a key role in modulating early events in wound healing; interaction of macrophages with dental implant surfaces can be an important determinant of success of osseointegration (15). This study, using a murine macrophage cell line, J744A.1, explored secretion and expression of pro-inflammatory cytokines and chemokines as a function of TiO<sub>2</sub> nanotube surfaces of different diameters. The results demonstrate that macrophage adhesion and proliferation, cell morphology, secretion and expression of pro-inflammatory cytokines (TNF- $\alpha$ ) and chemokines (MCP-1 and MIP-1 $\alpha$ ) were affected by TiO<sub>2</sub> nanotube surfaces, especially of 80 nm TiO<sub>2</sub> nanotube.

Early stages after implant insertion are important as early events form the foundation of wound healing around dental constructs (14). Macrophages are present immediately after implantation and prior to bone formation at dental implant surfaces (1). They can produce a variety of pro-inflammatory cytokines and chemokines, which have an impact on bone formation and resorption. Cytokines and chemokines produced by macrophages play key roles in immunoregulatory and inflammatory processes (1,5). Generally, pro-inflammatory cytokines and chemokines such as TNF- $\alpha$ , MCP-1 and MIP-1 $\alpha$  have been associated with both delayed bone healing and pathogenic bone loss. Furthermore, concentration of

a single mediator can also affect outcome of a response (8). Different dental implant surfaces have been shown to induce different macrophage activation types and different levels of cytokine secretion (14,16). In this study, TiO<sub>2</sub> nanotube surfaces, especially of 80 nm TiO<sub>2</sub> nanotube have been shown to induce different macrophage activation and different secretion and expression of TNF- $\alpha$ , MCP-1 and MIP-1 $\alpha$ .

Macrophage phenotype can be characterized as pro-inflammatory (M1) or immunomodulatory and tissue remodelling (M2) (31). M1 cells, classically activated pro-inflammatory macrophages, secrete pro-inflammatory cytokines and chemokines such as IL-1 $\beta$ , IL-6, TNF- $\alpha$  and MCP-1. In contrast, M2 cells, alternatively activated, play a predominant role in suppression of inflammatory responses and in promotion of tissue repair and regeneration (31,32). Macrophages have remarkable plasticity that allows them to efficiently respond to environmental signals and change their phenotype. There is strong correlation between early macrophage response to implants and outcome of tissue remodelling. Increased numbers of M2 macrophages and higher ratios of M2:M1 macrophages in the implant site, are associated with more positive remodelling outcomes (33). In this study, results of macrophage behaviour, secretion and expression of cytokines and chemokines indicated that these cells may become dif-

ferently activated upon interaction with TiO<sub>2</sub> nanotube surfaces. The results imply that TiO<sub>2</sub> nanotube surfaces can induce more M2 macrophages, which contributes to rapid bone wound healing for dental implants with TiO<sub>2</sub> nanotube surfaces *in vivo*.

Although the mechanism(s) of enhanced macrophage function on TiO<sub>2</sub> nanotube surfaces is still under investigation, changes in both topography and chemistry after anodization, and subsequent treatment, could have influenced macrophage responses observed in this study. Several altered surface characteristics may be responsible. First, surface topography resulting from different anodization parameters could be a major factor influencing macrophage functions (13,19,20). The unique TiO<sub>2</sub> nanotube structures here provided more surface area and more reactive sites for initial protein interactions, which mediated macrophage adhesion (34). For example, fibronectin and vitronectin adsorb to implant surfaces and act as ligands for macrophages through RGD-integrin receptor domains (34). These ligand interactions with several others, are primary interactions between implant surface and macrophages, resulting in cytokine release (34). In this study, it is possible that the unique nanotube-like structures were the sites for preferential adsorption of proteins such as fibronectin and vitronectin that mediated macrophage adhesion and subsequent function. Second, surface chemistry changed after anodization and subsequent heat treatment. For example, Ercan *et al.* (30) found 80 nm TiO<sub>2</sub> nanotubes had highest ratios of Ti/O compared to unanodized titanium. Yao *et al.* (35) provided evidence that anodized titanium had lower carbon content than unanodized titanium. Equally as important, F and N content were different between unanodized and anodized titanium (20,35). Third, anatase titanium dioxide surfaces are known to acquire photocatalytic properties under ultraviolet irradiation. Photocatalytic titanium dioxide surfaces are now thought to have various qualities such as bactericidal activity, decontamination capability, and hydrophilicity (36,37). Amorphous TiO<sub>2</sub> nanotubes can be transformed into anatase TiO<sub>2</sub> nanotubes after heat treatment. Photocatalytic anatase TiO<sub>2</sub> exhibits enhanced initial cell behaviour and early bone formation (38,39). Thus, all TiO<sub>2</sub> nanotube samples in this study were annealed at 450 °C after anodization to obtain anatase TiO<sub>2</sub> nanotube surfaces, and were sterilized by ultraviolet irradiation. Finally, changes in topography (35), heat treatment (40) and sterilization method (41) could also affect surface wettability and surface potential, which are known to influence cell responses. Cells preferentially attach to surfaces with higher surface energy (42). In our study, TiO<sub>2</sub> nanotube surfaces were more hydrophilic, thus of

higher surface energy. All these changes affected macrophage function. Other studies have shown that nanotopographical surface modification has resulted in marked down-regulation of the pro-inflammatory macrophage genotype compared to conventional microrough surface (11,19); this is consistent with the current study. Results of cell adhesion, proliferation and cell morphology here were consistent with those by Sun *et al.* (21), but the results of cell adhesion were different from those of Rajyalakshmi *et al.* (20). This is most likely attributable to the fact that they used a different macrophage cell line, different crystallinity of the TiO<sub>2</sub> nanotubes and the different testing methods.

In our study, the 80 nm TiO<sub>2</sub> nanotube surface provided good adhesion and proliferation support for macrophages and reduced protein secretion and mRNA expression of pro-inflammatory cytokines and chemokines compared to 30 nm TiO<sub>2</sub> nanotube surface. Also, these results can be explained by the following: First, the different nanotube sizes. On TiO<sub>2</sub> nanotubes, protein aggregates adhere to the upper wall surface owing to presence of empty nanotube pore spaces and gaps between adjacent nanotubes. It is possible that 80 nm TiO<sub>2</sub> nanotubes provided more appropriate sites for preferential adsorption of proteins that mediated macrophage adhesion and subsequent function. Second, the 80 nm TiO<sub>2</sub> nanotube structure is discrete with a gap between adjacent nanotubes (see Figs 1,2). Such a sub-division structure is important for minimizing interfacial stresses between two dissimilar materials contacted together. Third, gaps present between adjacent 80 nm TiO<sub>2</sub> nanotubes may also be useful as pathways for supply of nutrients – an essential biological element for cell growth (23).

In conclusion, in the current study we have shown that TiO<sub>2</sub> nanotube surfaces, especially of 80 nm TiO<sub>2</sub> nanotube, benefited macrophage adherence and proliferation and reduced protein secretion and mRNA expression of pro-inflammatory cytokines (TNF- $\alpha$ ) and chemokines (MCP-1 and MIP-1 $\alpha$ ). Therefore, it can be concluded that TiO<sub>2</sub> nanotube surfaces, especially of 80 nm TiO<sub>2</sub> nanotube, reduced the inflammatory response *in vitro*, which might be part of a basis for rapid osseointegration in implants with TiO<sub>2</sub> nanotube surfaces in animal studies.

## Acknowledgements

This work was supported by the National Natural Science Foundation of China (81171004, 81300916), Beijing Municipal Commission of Education Technology Innovation Platform (PXM2011\_014226\_07\_000065), and Capital Medical Development and Research Foundation of China (2009-3142).



## References

- 1 Terheyden H, Lang NP, Bierbaum S, Stadlinger B (2012) Osseointegration – communication of cells. *Clin. Oral Implants Res.* **23**, 1127–1135.
- 2 Lamers E, Walboomers XF, Domanski M, Prodanov L, Melis J, Luttge R, *et al.* (2012) In vitro and in vivo evaluation of the inflammatory response to nanoscale grooved substrates. *Nanomedicine* **8**, 308–317.
- 3 Waldeck H, Wang X, Joyce E, Kao WJ (2012) Active leukocyte detachment and apoptosis/necrosis on PEG hydrogels and the implication in the host inflammatory response. *Biomaterials* **33**, 29–37.
- 4 Scisłowska-Czarnecka A, Menaszek E, Szaraniec B, Kolaczowska E (2012) Ceramic modifications of porous titanium: effects on macrophage activation. *Tissue Cell* **44**, 391–400.
- 5 Brown BN, Ratner BD, Goodman SB, Amar S, Badylak SF (2012) Macrophage polarization: an opportunity for improved outcomes in biomaterials and regenerative medicine. *Biomaterials* **33**, 3792–3802.
- 6 Champagne CM, Takebe J, Offenbacher S, Cooper LF (2002) Macrophage cell lines produce osteoinductive signals that include bone morphogenetic protein-2. *Bone* **30**, 26–31.
- 7 Takebe J, Champagne CM, Offenbacher S, Ishibashi K, Cooper LF (2003) Titanium surface topography alters cell shape and modulates bone morphogenetic protein 2 expression in the J774A.1 macrophage cell line. *J. Biomed. Mater. Res. A* **64**, 207–216.
- 8 Szpaderska AM, Zuckerman JD, DiPietro LA (2003) Differential injury responses in oral mucosal and cutaneous wounds. *J. Dent. Res.* **82**, 621–626.
- 9 Chen S, Jones JA, Xu Y, Low HY, Anderson JM, Leong KW (2010) Characterization of topographical effects on macrophage behavior in a foreign body response model. *Biomaterials* **31**, 3479–3491.
- 10 Barrientos S, Stojadinovic O, Golinko MS, Brem H, Tomic-Canic M (2008) Growth factors and cytokines in wound healing. *Wound Repair Regen.* **16**, 585–601.
- 11 Hamlet S, Ivanovski S (2011) Inflammatory cytokine response to titanium chemical composition and nanoscale calcium phosphate surface modification. *Acta Biomater.* **7**, 2345–2353.
- 12 Schutte RJ, Parisi-Amon A, Reichert WM (2009) Cytokine profiling using monocytes/macrophages cultured on common biomaterials with a range of surface chemistries. *J. Biomed. Mater. Res. A* **88**, 128–139.
- 13 Mendonca G, Mendonca DBS, Aragao FJL, Cooper LF (2008) Advancing dental implant surface technology – from micron-to nanotopography. *Biomaterials* **29**, 3822–3835.
- 14 Refai AK, Textor M, Brunette DM, Waterfield JD (2004) Effect of titanium surface topography on macrophage activation and secretion of proinflammatory cytokines and chemokines. *J. Biomed. Mater. Res. A* **70**, 194–205.
- 15 Tan KS, Qian L, Rosado R, Flood PM, Cooper LF (2006) The role of titanium surface topography on J774A.1 macrophage inflammatory cytokines and nitric oxide production. *Biomaterials* **27**, 5170–5177.
- 16 Hamlet S, Alfarsi M, George R, Ivanovski S (2012) The effect of hydrophilic titanium surface modification on macrophage inflammatory cytokine gene expression. *Clin. Oral Implants Res.* **23**, 584–590.
- 17 Dalby MJ, Gadegaard N, Tare R, Andar A, Riehle MO, Herzyk P, *et al.* (2007) The control of human mesenchymal cell differentiation using nanoscale symmetry and disorder. *Nat. Mater.* **6**, 997–1003.
- 18 Wojciak-Stothard B, Curtis A, Monaghan W, MacDonald K, Wilkinson C (1996) Guidance and activation of murine macrophages by nanometric scale topography. *Exp. Cell Res.* **223**, 426–435.
- 19 Ainslie KM, Tao SL, Popat KC, Daniels H, Hardev V, Grimes CA, *et al.* (2009) In vitro inflammatory response of nanostructured titania, silicon oxide, and polycaprolactone. *J. Biomed. Mater. Res. A* **91**, 647–655.
- 20 Rajyalakshmi A, Ercan B, Balasubramanian K, Webster TJ (2011) Reduced adhesion of macrophages on anodized titanium with select nanotube surface features. *Int. J. Nanomedicine* **6**, 1765–1771.
- 21 Sun SJ, Yu WQ, Zhang YL, Jiang XQ, Zhang FQ (2013) Effects of TiO<sub>2</sub> nanotube layers on RAW 264.7 macrophage behaviour and bone morphogenetic protein-2 expression. *Cell Prolif.* **46**, 685–694.
- 22 Gong DW, Grimes CA, Varghese OK, Hu WC, Singh RS, Chen Z (2001) Titanium oxide nanotube arrays prepared by anodic oxidation. *J. Mater. Res.* **16**, 3331–3334.
- 23 Oh S, Daraio C, Chen LH, Pisanic TR, Finones RR, Jin S (2006) Significantly accelerated osteoblast cell growth on aligned TiO<sub>2</sub> nanotubes. *J. Biomed. Mater. Res. A* **78**, 97–103.
- 24 Popat KC, Leoni L, Grimes CA, Desai TA (2007) Influence of engineered titania nanotubular surfaces on bone cells. *Biomaterials* **28**, 3188–3197.
- 25 Park J, Bauer S, von der Mark K, Schmuki P (2007) Nanosize and vitality: TiO<sub>2</sub> nanotube diameter directs cell fate. *Nano Lett.* **7**, 1686–1691.
- 26 Oh S, Brammer KS, Li YSJ, Teng D, Engler AJ, Chien S, *et al.* (2009) Stem cell fate dictated solely by altered nanotube dimension. *Proc. Natl. Acad. Sci. USA* **106**, 2130–2135.
- 27 Bjursten LM, Rasmusson L, Oh S, Smith GC, Brammer KS, Jin S (2010) Titanium dioxide nanotubes enhance bone bonding in vivo. *J. Biomed. Mater. Res. A* **92**, 1218–1224.
- 28 Wang N, Li H, Lü W, Li J, Wang J, Zhang Z, *et al.* (2011) Effects of TiO<sub>2</sub> nanotubes with different diameters on gene expression and osseointegration of implants in minipigs. *Biomaterials* **32**, 6900–6911.
- 29 von Wilmsow C, Bauer S, Roedel S, Neukam FW, Schmuki P, Schlegel KA (2012) The diameter of anodic TiO<sub>2</sub> nanotubes affects bone formation and correlates with the bone morphogenetic protein-2 expression in vivo. *Clin. Oral Implants Res.* **23**, 359–366.
- 30 Ercan B, Taylor E, Alpaslan E, Webster TJ (2011) Diameter of titanium nanotubes influences anti-bacterial efficacy. *Nanotechnology* **22**, 295102.
- 31 Franz S, Rammelt S, Scharnweber D, Simon JC (2011) Immune responses to implants – a review of the implications for the design of immunomodulatory biomaterials. *Biomaterials* **32**, 6692–6709.
- 32 Brown BN, Valentin JE, Stewart-Akers AM, McCabe GP, Badylak SF (2009) Macrophage phenotype and remodeling outcomes in response to biologic scaffolds with and without a cellular component. *Biomaterials* **30**, 1482–1491.
- 33 Brown BN, Londono R, Tottey S, Zhang L, Kukla KA, Wolf MT, *et al.* (2012) Macrophage phenotype as a predictor of constructive remodeling following the implantation of biologically derived surgical mesh materials. *Acta Biomater.* **8**, 978–987.
- 34 Jakobsen SS, Larsen A, Stoltenberg M, Bruun JM, Soballe K (2007) Effects of as-cast and wrought Cobalt-Chrome-Molybdenum and Titanium-Aluminium-Vanadium alloys on cytokine gene expression and protein secretion in J774A.1 macrophages. *Eur. Cell Mater.* **14**, 45–54.

- 35 Yao C, Slamovich EB, Webster TJ (2008) Enhanced osteoblast functions on anodized titanium with nanotube-like structures. *J. Biomed. Mater. Res. A* **85**, 157–166.
- 36 Wang R, Hashimoto K, Fujishima A, Chikuni M, Kojima E, Kitamura A, *et al.* (1997) Light-induced amphiphilic surfaces. *Nature* **388**, 431–432.
- 37 Jimbo R, Sawase T, Baba K, Kurogi T, Shibata Y, Atsuta M (2008) Enhanced initial cell responses to chemically modified anodized titanium. *Clin. Implant Dent. Relat. Res.* **10**, 55–61.
- 38 Sawase T, Jimbo R, Baba K, Shibata Y, Ikeda T, Atsuta M (2008) Photo-induced hydrophilicity enhances initial cell behavior and early bone apposition. *Clin. Oral Implants Res.* **19**, 491–496.
- 39 Hirakawa Y, Jimbo R, Shibata Y, Watanabe I, Wennerberg A, Sawase T (2013) Accelerated bone formation on photo-induced hydrophilic titanium implants: an experimental study in the dog mandible. *Clin. Oral Implants Res.* **24**(Suppl A100), 139–144.
- 40 Shin DH, Shokuhfar T, Choi CK, Lee SH, Friedrich C (2011) Wettability changes of TiO<sub>2</sub> nanotube surfaces. *Nanotechnology* **5**, 315704.
- 41 Zhao L, Mei S, Wang W, Chu PK, Wu Z, Zhang Y (2010) The role of sterilization in the cytocompatibility of titania nanotubes. *Biomaterials* **31**, 2055–2063.
- 42 Zhao G, Schwartz Z, Wieland M, Rupp F, Geis-Gerstorfer J, Cochran DL, *et al.* (2005) High surface energy enhances cell response to titanium substrate microstructure. *J. Biomed. Mater. Res. A* **74**, 49–58.